Rapid and effective method of laser metallization of dielectric materials using deep eutectic solvents with copper acetate

Evgeniia Khairullina[1], Andrey Shishov[1], Dmitry Gordeychuk[1], Lev Logunov[2], Aleksandra Levshakova[1], Vladimir B. Sosnovsky[1], Aleksandra Koroleva[1], Vladimir Mikhailovsky[1], Evgeny Gurevich[4], Ivan Chernyshov[3], Maxim Panov[1], Ilya Tumkin[1]*

[1] - Saint Petersburg State University, 7/9 Universitetskaya nab., St. Petersburg 199034, Russia
[2] - School of Physics and Engineering, ITMO University, Lomonosova, 9, Saint-Petersburg, 191002, Russia
[3] – TheoMAT group, ChemBio cluster, ITMO University, Lomonosova, 9, Saint-Petersburg, 191002, Russia
[4] - Laser Center (LFM), University of Applied Sciences Münster, Stegerwaldstraße 39, 48565 Steinfurt, Germany
*Corresponding author e-mail: i.i.tumkin@spbu.ru

Abstract
In this paper, we proposed rapid laser-induced synthesis of copper micropatterns on the surface of oxide glass from deep eutectic solvents (DESs) consisting of choline chloride, citric or tartaric acid and copper acetate as copper plating solutions. It was shown that upon irradiation with continuous-wave 532-nm laser radiation, it is possible to increase the deposition rate of copper and create micropatterns with a resistance close to the value of pure metal together with high adhesion to the substrate surface. This metallization method is favorable for the practical use of copper patterns, including in production of new printable microelectronic devices. Thus, we demonstrated the possibility of copper deposition on arbitrary three-dimensional surfaces. Moreover, the resulting copper micropatterns were tested as working electrodes for non-enzymatic glucose. Finally, the proposed technology can be successfully used for design and development of sensor platforms for the electrochemical analysis and microelectronic devices.

Keywords: direct laser writing, copper, sensors, deep eutectic solvents, laser processing, microelectronics

Introduction

The development of new methods appropriate for fabrication of the conductive micropatterns (circuits) is rather important for the electronic device production and science. Traditionally, lithography technology is widely applied in the printing circuit board industry for manufacturing its circuits [1]. However, this approach is time-consuming and expensive, involving many steps such as etching and electroplating. In addition, since a solvent used in the etching process is corrosive, the choice of a substrate is limited, so that it can be not applicable for e. g. printable electronics on flexible substrate and roll-to-roll production. As a result, there has been a lot of interest in recent years in developing effective and low-cost processing techniques for fabricating conductive patterns. Methods of maskless direct laser writing are considered as a promising alternative to the traditional lithography and other existing technologies for production of the microelectronic components, sensors and other devices [2]–[4]. Laser-assisted methods can be divided into two groups. The *first group* includes technologies, in which laser radiation is used as a preliminary activation or sensitization of the surface. For example, selective surface activation induced by laser (SSAIL) is among these methods, in which it is possible to create copper micropatterns on almost any surface of polymers and rigid dielectrics using laser activation by ps pulses and subsequent chemical reduction process [5]–[7]. Another example from the first group is laser activation with simultaneous chemical sensibilization of the surface using organic

precursors [8], [9]. Despite the high metallization rate associated with these approaches, laser methods that utilize a single-stage metallization process are currently gaining a lot of attention. Indeed, it can significantly reduce the consumption of expensive reagents and reduce the manufacturing time. Thus, such single-stage techniques can be included in the *second group* of laser methods. In the second approach, a precursor containing a metal source is placed in a solution or coated on the surface of a substrate and irradiated by laser. As a result, metal micropatterns are formed within the area of laser exposure and the laser beam performs the function of a "pen". Among the main advantages of such methods is the possibility of local creation of microstructures on almost any surface. Selective laser sintering (SLS) is a vivid example of such methods, in which the metallic powder is layer-by-layer exposed to laser irradiation. SLS enables the selective creation of copper and nickel structures on the surface of polymers and other materials. [4], [10], [11]. However, the development of SLS faces several challenges, including the high cost and difficulty of preparing the precursor, as well as the requirement of using non-environmentally friendly solvents to remove the unreacted material. For this reason, method of laser-induced chemical liquid-phase deposition of metals from solution (LCLD) seems particularly attractive. In this method, a metal reduction reaction occurs on the surface of a substrate within the focus of the laser beam leading to formation of various types of porous metal microstructures [12]–[15]. Thereby, LCLD allows to synthesize electrocatalytically active metallic and bimetallic microstructures based on various metals, including copper and gold that are suitable for enzyme-less sensing of glucose, hydrogen peroxide and other biologically important analytes [16]. LCLD has a number of advantages: it is quite easy to use, it does not require expensive equipment and it is versatile and cheap. Additionally, LCLD can be utilized for depositing metal structures onto various surfaces, including glass, ceramics, and polymers. [17]. However, this technique also exhibits several significant shortcomings. At first, there is an uncontrollable defocusing of the laser beam leading to a change in the morphology of the depositing metal structures. This is caused by the formation of gas bubbles at the phase interface within the localized boiling points of the solution. Another drawback is the slow rates of metal deposition from both aqueous and organic solutions.. In this case, the average deposition rate is approximately 0.01 mm per second that results in an excessive duration of the deposition process. The main characteristics of the aforementioned methods are summarized in the table 1.

Table 1. Comparison of different laser fabrication techniques.

Method	**Laser type**	**Feature size/ widths of micropatterns [µm]**	**Scanning speed, [µm s−1]**	**Deposited metals**	**Substrate**	**Number of experimental steps**	**Limitations/crucial requirements**	**References**
Laser-induced photoreduction	continuous, pulsed	0.2/0.4	1–100	Au, Ag	glass	1	photoactive precourses	[18]–[20]
LIFT	pulsed	1-7	3.0 × 10−2	Cu, Au, Ag, Al, Cu, V, Cr, Ti, Ge, Sn, W, Pd, Ni, Zn,	metals, polymers, ceramics, glass, paper	2	positioning of donor and acceptor substrate with high precision	[21]–[23]

				Pt, Au-Sn, Ge-Sn				
SLS	cw, pulsed	10	1000	Au, Ag, Pt, Cu, Ni, Co	ceramics, glass, polymers	2	resynthesized nanoparticles	[24]–[26]
SSAIL	pulsed	25	До 6*10^6	Cu	ceramics, glass, polymers	3	ps laser for substrate activation	[6], [27], [28]
LCLD	continuous, pulsed	20	0.5	Au, Ag, Ni, Cu, Ru, Ir, Pt	ceramics, glass	1	thermostable substrates	[29]–[31]
LCLD + DES	continuous, pulsed	20	2500	Cu, Ni, Co, Ni-GO	glass	1	thermostable substrates	[32]–[34]

In contrast, in the current work, we used deep eutectic solvents (DESs) instead of solutions typically utilized in LCLD. As a result, it allows to significantly simplify the metal deposition procedure and increase the deposition rate of metals by more than a factor of 150. In general, DES is a mixture of two or more substances whose melting point is lower than that of the individual components of this mixture [35]. In addition, it is known that DESs are effective solvents for metal salts [36].

The continuously increasing number of publications highlights the potential of using deep eutectic solvents (DES) as valuable alternatives to organic solvents and ionic liquids. DES has a number of advantages that make their application particularly interesting for the LCLD method. For instance, DESs exhibit higher electrochemical and thermal stability compared to aqueous and organic solutions, which enables their use over a wide temperature range [37]. DESs have a high enough viscosity to be used as thin coating films on the surface of the substrates for further laser irradiation. This advantage allows to significantly reduce the consumption of the reagents. In addition, DESs are traditionally referred to “green chemistry”, since only environmentally friendly and safe substances are used in their preparation. Therefore, DES can be considered as the promising solvents for the deposition of metals under the action of laser radiation. In our previous works, we optimized physical and chemical factors affecting the process of the formation of copper and nickel micropatterns [34]. It was shown that micropatterns with a high copper content can be fabricated using systems based on choline chloride, copper chloride and organic acids (citric or tartaric) [33].

In this paper, we propose an approach which allows to fabricate micro-dimensional patterns not only on flat dielectric substrates, but also on non-planar samples. Thus, we performed laser-induced deposition from a DES-based solution with dissolved copper acetate as a metal source. The effectiveness of this approach was approved by its high rate, which is 100-200 times higher than those observed for LCLD in aqueous solutions [38]. In turn, this may be useful for the technological application of this technique.

In addition, we provide a mechanism explaining the process that occurs under the action of laser radiation and leads to the formation of the metallic deposits. It was also performed a comparative characterization and measurement of the current-voltage parameters of copper micropatterns fabricated using citric and tartaric acids as proton donors. The applicability of the obtained copper

micropatterns was shown by the electrochemical studies, where these structures were used as working electrodes for non-enzymatic sensing of glucose and other analytes. It was also demonstrated that the synthesized materials could be used to create microelectronic devices based on LED.

2. Experimental

2.1. Reagents, solutions and materials

Choline chloride, $Cu(CH_3COO)_2 \times 2H_2O$, oxalic, citric, tartaric, and succinic acids were purchased from Sigma Aldrich and used as received. Glass substrates were purchased from Levenhuk. Glass ampoules with a radius of 11.35 mm were chosen as non-planar surfaces, the ampoules were cutted with a glass cutter in two halves and the DES was applied on the inner surface of the side wall.

2.2. Preparation of Cu salt ink

The necessary weights of choline chloride, acid and copper salt were mixed in 10 mL glass vials. The ratio of acid to choline was always kept to 1:1 mol/mol. The mass of copper salt was varied. Then, the vials were placed in a drying cabinet at a temperature of 120 °C. After the mixture began to melt, it was placed on a magnetic heating stirrer, a magnetic stirrer bar was placed in the vials and mixed at 120-140 °C until viscous homogeneous liquids were obtained. Before placing it on the surface of a substrate, the prepared DESs were heated in drying cabinet (50-60oC) to decrease viscosity.

2.3. Coating method and laser reduction

The surface activation was carried out for 10 minutes in the “reactive ion etching” (RIE) mode at full power (450 W) in the YES-G500 plasma (Ar, 6.0, 26 sccm + O2, 5.0, 26 sccm) cleaning unit (Yield Engineering Systems, Inc.). The authors in [3] showed that plasma surface treatment has a positive effect on the adhesion of the solution to a substrate due to a change in the wetting angle of the substrate surface. It also positively affects the adhesion of the forming metal micropatterns.

The blade spreading method was used to place the DES on the glass surface. As a result, the optimal film thickness of 1 mm was chosen. A continuous wave (CW) 532 nm diode-pumped solid state Nd:YAG laser (Changchun, China) was utilized to obtain conductive structures. A standard microscope objective with a focal length of 15 mm was used to focus the laser beam and the diameter of the irradiated zone was approximately 50 μm. The power of the laser radiation varied with the range between 0,25-1,5 W. The scanning speed of the laser beam was varied from 0.0025 to 25 mm s^{-1}. Fabrication of copper micropatterns using laser irradiation was carried out according to the following scheme. The substrate with DES was scanned with a laser beam from the reverse side to avoid splashing (i.e. through the glass substrate). The substrate was fixed vertically and moved using the motorized XYZ-stage. The details of this scheme can be found elsewhere [33]. The unreacted solution was washed off with water after laser patterning (Fig. S1 a,b in the supplement). As has been mentioned, in many methods of direct laser writing, such as SLS, it is necessary to remove the traces of an unreacted solution after exposure to a laser beam. This was achieved in [11] by using solvents, which are components of DES. Thus, in our case, the unreacted DES was removed using water, since the composition of DES used is water-soluble. Further, the fabricated copper micropatterns were washed in dilute sulfuric acid for 10 min in order to remove possible impurities from their surface. The selection of the optimal solvent for removing the unreacted DES and cleaning the surface of the formed metal micropatterns has also been carried

out. For this purpose, several solvents of different nature were tested: acetone, ethanol, water, etc. The results indicated that hot water (80-90 °C) is the most effective solvent for cleaning and removing any unreacted solution.

Deep eutectic solvents vary significantly in viscosity depending on the composition (from 100 to 100000 MPa s) while it was shown that DES with high fluidity cannot be used. Indeed, in this case, the scanning laser beam locally reduces the viscosity at the point of exposure and nearby zones, which leads to the spreading of the solution and stopping the laser-induced reaction. On the other hand, for DESs with low viscosity a preliminary short-term heating (3-10 min) of a substrate with the DES film at a temperature not higher than 150 ^{o}C, depending on the composition of a solvent was proposed before laser synthesis. This process results in the partial removal of water and an increase in viscosity, enabling the conduct of laser-induced synthesis in such systems. We attribute this effect to the creation of activation centers in the form of partially reduced copper when the solution is heated. Figure 1 illustrates copper patterns obtained with and without substrate preheating prior to laser exposure from solution **4**.

2.4. Physical and chemical characterization

The morphology of the fabricated copper structures was investigated using scanning electron microscopy (SEM). The atomic composition of these microdeposits was studied using energy dispersion of X-ray spectroscopy (EDX). The EDX-system was coupled with a Zeiss Supra 40 VP scanning electron microscope equipped with X-ray attachment (Oxford Instruments INCA X-act). The X-ray diffraction (XRD) analysis was performed for identification of the crystallization phase of the obtained copper structures. The copper microstructures with a size of 5 by 3 mm was deposited from the solutions with compositions listed in Table 1 in order to perform X-ray phase analysis. The XRD patterns were recorded on a Bruker D2 Phaser diffractometer equipped with LynxEye detector using CuKα radiation in the 2θ angle range of 0^{o}-100^{o}.

The X-ray photoelectron spectroscopy (XPS) was used to study the elemental composition, chemical and electronic state of atoms on the surface of the copper patterns. The XPS analysis was done using the photoelectron spectrometer “Escalab 250Xi” with AlKα radiation. All spectra were collected in the constant pass energy mode at 50 eV for element core level spectrum and 100 eV for survey spectrum (spot size 650 μm).

In order to measure the electrical resistance, the metal contacts were sprayed onto the edges of the fabricated materials using ion vacuum spraying (Gatan PECS). Silver was used as the contact material. The thickness of the sprayed contacts was 200 nm. The measurement of the voltammetric characteristics was carried out using the Stanford Current Meter RS 570. The voltage range was limited to the maximum measured current (5.8 mA).

2.5. Electrochemical measurements

Electrocatalytic performance of the synthesized copper micropatterns toward non-enzymatic sensing of D-glucose and hydrogen peroxide was tested using voltammetric techniques at room temperature in a standard three-electrode cell. In this cell, copper deposits were used as working electrodes, whereas platinum wire and Ag/AgCl electrode were used as counter and reference electrodes, respectively. Amperograms and cyclic voltammograms (CV) were recorded in 0.1 M NaOH using Corrtest CS300 potentiostat (Woham Corrtest Instruments Ltd., China).

2.6. Computational methods

All quantum chemical calculations were performed using the Orca program package [39]. Geometries of reagents and transition states were calculated at the PBE0-D3/6-311G(d,p)/CPCM level of theory. Water and DMF were used as solvents due to the unavailability of CPCM parametrization for DESs. The nature of local minima was confirmed by frequency calculation. Implicit solvent models cannot be used to describe dissociation of strong acids in water without explicit consideration of the solvation shell, thus we used experimental value of H+ solvation free energy [40].

3. Results and discussion

3.1. Optimization of laser irradiation parameters

The copper microstructures with a size of 5 by 3 mm was deposited from the solutions shown in Table 2 in order to determine the optimal parameters of laser irradiation and the scanning speed. Depending on the composition of the solution and irradiation parameters, we obtained micropatterns with the electrical resistance varied from 5 to 100 Ω (more detailed discussion of electrical resistance is presented in section 3.4 *Investigation of current-voltage characteristics)*. It was shown that copper micropatterns with an electrical resistance close to pure copper are formed only from solutions containing tartaric or citric acid. This result is in agreement with those observed in the work on optimizing the parameters for laser deposition from DES [33] with copper chloride salt as a precursor.

Table 2. Compositions of DESs

solution / component, mol ratio	1	2	3	4
choline chloride	1	1	1	1
copper acetate	1.5	3	1.5	3
tartaric acid	-	-	1	1
citric acid	1	1	-	-

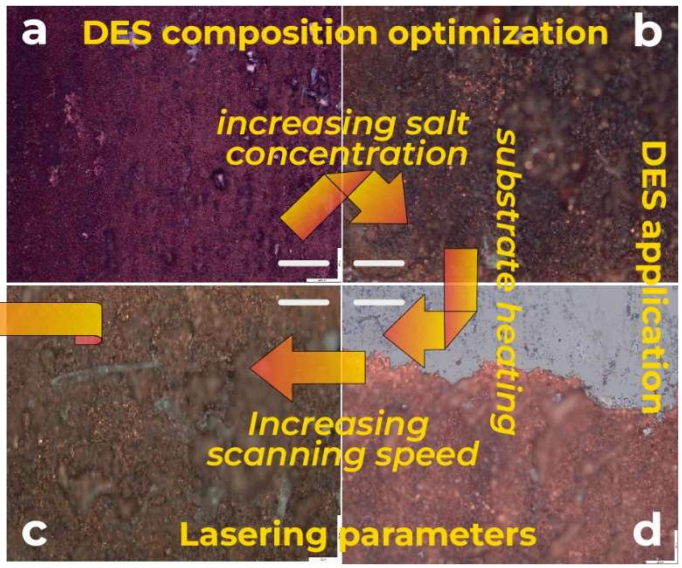

Fig. 1. Compositions of DESs used for laser synthesis of copper micropatterns. (a)-(d) Optical micrographs of copper structures synthesized at scanning speeds of 2.5 mm/s and 0.25 mm/s, with and without substrate heating (e) Photographs of copper patterns deposited on a three-dimensional surface and a demonstration of the operability of these structures.

The power range of laser radiation for solutions **1**-**4** was varied between 0,5 and 1W. Thus, conductive copper micropatterns were obtained from solutions **2** and **4** at scanning speeds of 0.25 mm/s and 2.5 mm/s. The morphology characterization and elemental analysis of the fabricated micropatterns at laser power of 1 W and the scanning speed of 2.5 mm/s were performed using SEM and EDX, respectively. The morphologies of the structures deposited from solution 2 and 4 are quite similar. However, the XRD analysis (Fig. 2) demonstrated that these patterns fabricated

with solution 4 mainly consist of copper with an insignificant amount of copper (I) oxide, while the structures produced from DES 2 contain a noticeable amount of impurities (copper(I) oxide, copper (I) chloride). It was shown that washing the fabricated materials in a dilute solution of sulfuric acid (0.01 M) for 12 hours is quite effective method for cleaning the surface from by-products, while not disturbing the initial topology of the deposit (Fig. S3). The presence of copper in the sample was also confirmed by XPS analysis (Fig. 2g). The spectrum also exhibits strong satellites characteristic of the Cu^{2+} state. On the other hand, the second state, characterized by the lowest binding energy 932.5 eV, can be defined as metallic copper Cu^0 released as a result of the reduction reaction. The presence of Cu^{2+} in XPS spectrum can be explained by interaction of the metallic copper with oxygen of the atmosphere.

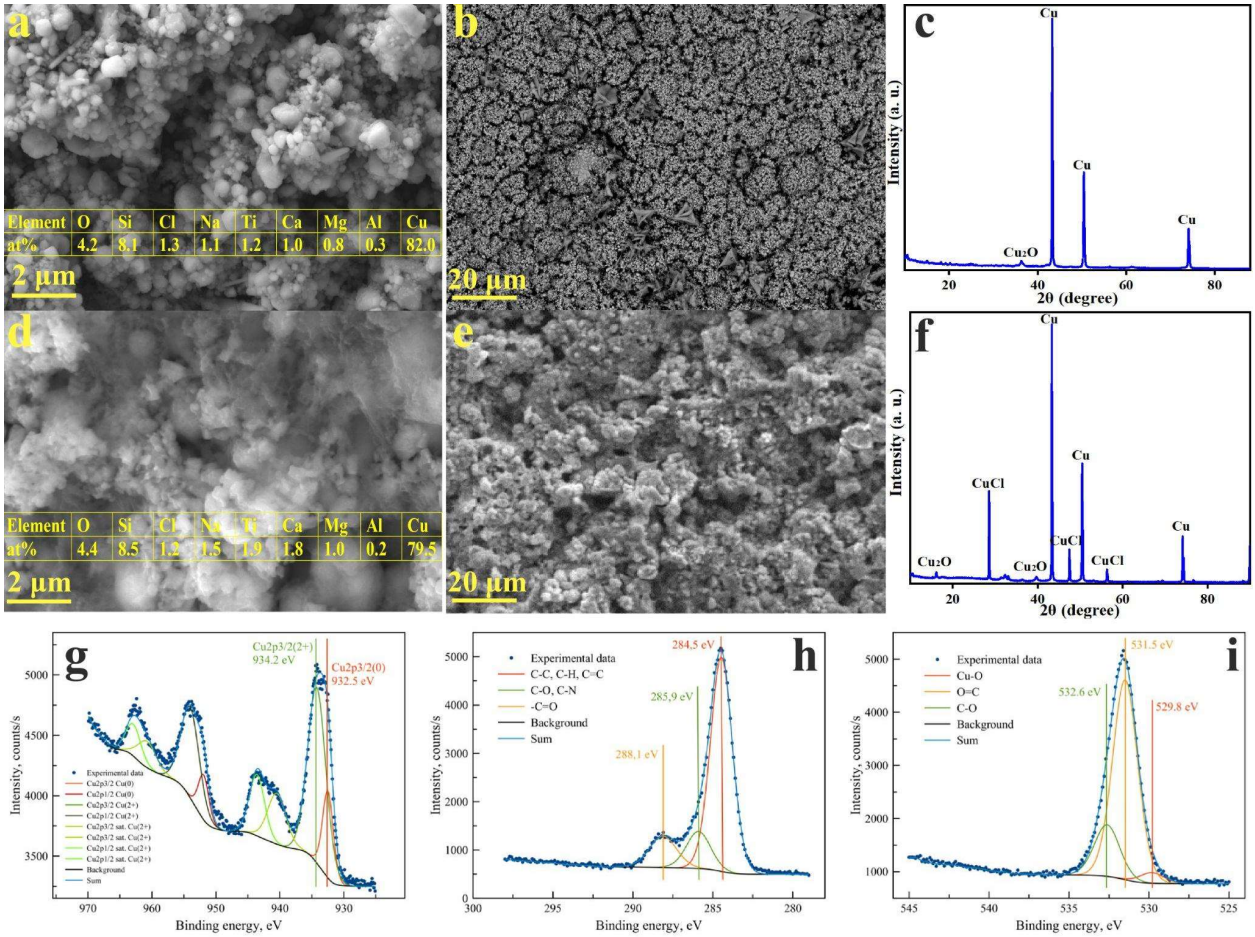

Fig. 2. (a, b) SEM images of copper micropatterns deposited from solution 4 (containing tartaric acid) on oxide glass surface. (c) XRD analysis of copper micropatterns deposited from solution 4. (d, e) SEM images of copper micropatterns deposited from solution 2 (containing citric acid) onto the oxide glass surface. (f) XRD analysis of copper micropatterns deposited from solution 2. (g, h, i) XPS of copper micropatterns deposited from solution 4. Tables at (a) and (d) show the results of the edx analysis.

It should be noted that a similar result was obtained for a solution containing tartaric and citric acids with copper chloride used as a source of copper. The mechanism of influence of acids was described in [33]. We attribute a significant improvement in properties of copper micropatterns, including morphology and electrical conductivity, to the use of copper acetate instead of inorganic copper salt. It seems that the influence of the form of copper in the DES is significant. Indeed, in

our previous work, we implemented copper (II) chloride, which was used in the form of crystallohydrate with six water molecules [33]. In contrast, copper acetate used in the current work exists in the form of crystallohydrate with two water molecules. The smaller the number of water molecules in DES, the higher viscosity of DES and higher its adhesion to a substrate. The latter leads to more stable layers of DES on the surface. In turn, this effect is partially leveled by preliminary short-term heating of the DES film. On the other hand, copper acetate is undergoes to thermal decomposition and when it is used, the process of laser thermal reduction of copper on the surface of non-conductive materials is more easily initiated. However, this mechanism is apparently not the only one that leads to the reduction of copper ions and the deposition of metal structures on the substrate surface upon laser irradiation.

To explain the mechanism of formation of copper micropatterns under the action of laser radiation, the following considerations were discussed. A simple estimation of the DES temperature induced by the laser radiation gives a surprisingly deep insight into possible physical mechanisms of the formation of the metal structures. We do this estimation based on a simple energy balance: the energy of the laser light increases the temperature of the DES in the volume, which is defined by the laser light absorption and the thermal conductivity. This volume will be estimated first. Some of the material and optical parameters for DES are not known exactly and cannot be measured precisely; in this case, we take the values, which give us the lowest possible temperature in the estimation. After estimating the DES temperature we analyze whether this temperature is feasible: if not, the model should be corrected.

(1) Estimation of the heat-affected volume. The laser radiation is focused into a spot of approximately d=30 μm in diameter, the laser scanning speed is v=0.3 mm s^{-1}, hence the time interval during which the temperature of a particular point increases due to the laser heating can be estimated as $th=d/v$=0.1 s. The thermal conductivity of different DES is in the range λ_t=0.2-0.4 W/(m K) [27]. Estimating the thermal capacity of the DES as the thermal capacity of the main component (citric acid) $c_v\approx$0.7 J/(cm^3 K) we calculate the thermal diffusivity $\alpha= \lambda_t/c_v\approx$0.4 cm^2 s^{-1}. The width of the heat affected zone is than the distance, the heat diffuses during the time interval th, which can be calculated as $L\approx(\alpha*th)^{1/2}\approx$2 mm. We notice that this estimation is larger than the observed width (i.e. approx 100-150 μm) of the metal tracks that conforms that we have photo-thermal mechanism of the metal reduction. The absorption depth of the laser wavelength (λ=532 nm) can not be measured precisely but the layers are optically not transparent, hence the absorption depth is smaller than the DES layer thickness h (i.e. approx 1 mm). Hence, to get the lowest temperature the absorption depth is taken as h.

(2) Assuming that the initial temperature is close to the room temperature T_0 one can write:

$(T-T_0)\times c_v\times L\times hd=(1-R)\times P\times th$,

Here, R is the reflection coefficient of the DES, which is much smaller then 1, P is the laser power taken as P=1 W for this estimation. The result of the estimation made in the frames of this model is not realistic: T=2400 K, hence, there are other processes limiting the temperature increase. These additional mechanisms are not related to the substrate, because the substrate processes would influence the width of the metal tracks, which were well estimated in frames of the model. Hence, we assume a sort of self-regulation process upon the laser processing: as soon as metallic structure appears, the laser beam scattering and reflection increase and prevent the beam from further penetration into DES. Due to this mechanism, the laser power absorbed by the DES is self-limited and does not destroy the material at such a high average laser power.

In addition to local modification of the planar substrates, the possibility of copper deposition on arbitrary three-dimensional surfaces was shown. These materials can be used to create curved parts of various devices for the integration of conformal antennas and circuits, including RFID labels (Radio Frequency Identification), which are one of the foundations of the Internet of Things [43]. Moreover, they can be utilized for the production of epidermal wearable devices, [44], devices for monitoring the environment and food quality [45-46]. The non-planar synthesis was carried out taking into account the results obtained for planar substrates, a solution based on copper acetate and tartaric acid was used for deposition, it is worth noting that the scanning speed during deposition on three-dimensional surfaces is equal to that for planar. Fig. 1 shows a photograph of copper deposits. It is shown that they have a resistance close to the value of pure metal, as well as high adhesion to the surface. Thus, it is possible to use these copper patterns in practice, including for creating microelectronic devices based on LED [47-48]

Based on the literature data presented in Table 1 and our experimental findings, it can be concluded that optimized parameters of laser irradiation can achieve scanning speeds comparable to those of established techniques such as selective laser sintering (SLS).The proposed method offers a high level of overall productivity and can be matched even with methods that have higher scanning speeds but require additional time-consuming procedures (such as SSAIL), taking into account the minimal substrate pretreatment and experimental stages. Furthermore, the proposed laser chemical liquid deposition technique can be conducted using continuous wave lasers, which have a simple design compared to pulsed lasers.

3.2. Effect of copper precursor

Fig. S2 illustrates SEM micrographs of copper micropatterns deposited from solutions with different concentrations of copper acetate and tartaric acid of fixed concentration (solutions **1**, **2**). It has been experimentally determined that lowering the mole ratio of salt in relation to the other components below 1:0.5 leads to a deposit with numerous defects, which are associated with a lack of copper cations. The use of a higher content of copper acetate is impossible due to the unsatisfactory adhesion of DES to the substrate material. In turn, micropatterns obtained from compositions 1 (ChCl) : 1.5 (CuAc) : 1 (organic acid) and 1 : 3 : 1 have high electrical conductivity close to pure copper. In the process of optimizing the chemical composition of the used solutions, it was determined that in order to obtain the most copper-enriched (according to XRD data) patterns with a uniform structure (according to SEM data), it is necessary to use the composition with 1.5 mol or 3 mol. of copper acetate with fixed amount of choline chloride and organic acid (table 1).

We assume that the efficiency of copper acetate as compared to copper chloride is due to acetate ion acting as a base for the copper complexation by citric/tartaric acids, which is the first stage of the copper photoreduction process. Indeed, if copper chloride is used as a copper source, the strongest base in the resulting solution is water, and the reaction will lead to the accumulation of strong hydrochloric acid:

$$RCOOH + Cl–[Cu] \rightleftharpoons RCOO–[Cu] + HCl \quad (1)$$

On the contrary, acetate is a much more strong base as compared to water (pKa of the conjugated acids are -1.74 and 4.76, respectively), and thus acetate ions are in equilibrium with citrate or tartrate ions:

$$RCOOH + MeCOO– \rightleftharpoons RCOO– + MeCOOH \quad (2a)$$

Further, citrate/tartrate ion replace chloride in copper complexes significantly easier than the corresponding acid:

$$RCOO– + Cl–[Cu] \rightleftharpoons RCOO–[Cu] + Cl^- \quad (2b)$$

Therefore, the use of copper acetate leads to higher concentrations of citrate/tartrate copper complexes, resulting in higher efficiency of the photoreduction process.

To support this hypothesis, we used quantum chemical modeling to estimate the free energies of processes (1) and (2). The source of copper was modeled using the $[CuCl4]^{2–}$, which is one of the dominant Cu^{2+} forms in choline chloride-based DESs [49-50]. Acetic acid was used instead of citric and tartaric acids due to the close pKa values (3.1, 3.0, and 4.76 for citric, tartaric, and acetic acids, respectively) and the simplicity of the atomistic model. For the same reason, the proton exchange between acetic and citric/tartaric acids was not considered. Several possible forms of HCl were considered, including non-dissociated, dissociated to H^+ and Cl^-, and an $HCl^{2–}$ anion. Since there is no CPCM parametrization for any DES, DMF and water were used as solvents due to their high polarity and potential similarity with the considered DESs. Reactions selected for the theoretical modeling and the corresponding thermodynamical parameters are provided in Table 2.

Table 2. Theoretical electronic and free energies of the considered ligand exchange reactions, $kJ \cdot mol^{-1}$.

Eq.	Reaction	DMF		Water	
		ΔE	ΔG	ΔE	ΔG
(1)	$MeCOOH + [CuCl_4]^{2–} \rightleftharpoons [(MeCOO)CuCl_3]^{2–} + HCl$	70	68	70	68
(2)	$MeCOOH + [CuCl_4]^{2–} \rightleftharpoons [(MeCOO)CuCl_3]^{2–} + H^+ + Cl^-$	—	94	—	90
(3)	$MeCOOH + [CuCl_4]^{2–} + Cl^- \rightleftharpoons [(MeCOO)CuCl_3]^{2–} + [Cl\cdot\cdot H\cdot\cdot Cl]^-$	25	43	26	44
(4)	$MeCOO^- + [CuCl_4]^{2–} \rightleftharpoons [(MeCOO)CuCl_3]^{2–} + Cl^-$	-33	-11	-34	-14

As we can see from Table 2, reaction between $[CuCl_4]^{2–}$ and acetate is significantly more favorable for the copper acetate (reaction 4 in Table 2) as compared to the copper chloride (reaction 3 in Table 2): the corresponding theoretical free energies are -11 and 43 $kJ \cdot mol^{-1}$ in DMF, and -14 and 44 $kJ \cdot mol^{-1}$ in water.

3.4. Investigation of current-voltage characteristics

Dependency analysis shown in Fig. 3a demonstrates that all the characteristics have a linear form indicating a constant value of the electrical conductivity of the samples. The resistance of the samples can be estimated using the slopes of the straight line corresponding to I(V) dependence. The measured values of resistance are: 23 Ω for rectangles and 5.3 Ω for lines. The resistance of the copper lines turned out to be less than the resistance of the rectangular samples, probably, due to the presence of the initial gel solution, which can partially penetrate into the pores.

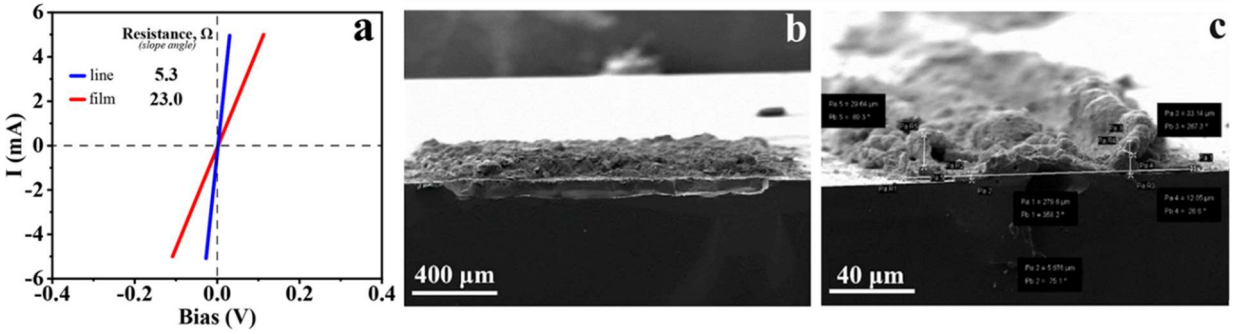

Fig. 3. (a) Current-voltage characteristics of the synthesized rectangular samples. SEM image of a transverse cross-section of a rectangular sample (b) and a line (c).

In addition, the increase in resistance values after synthesis and during the presented experiment can be explained by partial oxidation of the micropattern surface. These assumptions can be supported by the X-ray photoelectron spectroscopy (Fig. 2 g,h,i). Fig. 2 h,i show the deconvolution of the carbon and oxygen XPS spectra, respectively. Both spectra were deconvoluted into three Gaussian peaks. These peaks can be attributed to the presence on the sample surface of the natural adsorbates and the organic residues left after the cleaning. Moreover, the XPS signal with the lowest binding energy (529.8 eV) in Fig. 2i presumably arises due to oxidation reaction caused by the interaction between the formed metallic copper and air oxygen.

Next, the specific resistance of copper micropatterns was calculated. The thickness of the samples can vary from point to point, while its average value remains constant. Based on the SEM images of the transverse chips of the samples (Fig. 3 b), the following estimated values of the cross-section of the samples were obtained: rectangle – $2.1 \times 0.130 = 0.273$ mm^2; line – 0.28×0.005 mm^2 + $2 \times 0.03 \times 0.01$ mm^2 = 0.008 mm^2.

The geometric dimensions of the samples and the calculated values of their resistivity are presented in Table 4.

Table 4. Geometric dimensions of the samples and the calculated values of their resistivity.

Sample	Cross-section, mm^2	Specific resistance, Ω mm^2 m^{-1}
film	0.273	2100
line	0.008	8

It should be noted that the resistivity of monocrystalline copper is about 0.017 Ω mm^2 m^{-1}. The difference in resistivity (102-105 times) is presumably mainly due to the significant porosity of the fabricated samples, and, as a result, the significant length of the current flow channels, as well as possibly incomplete cleaning.

3.5. Investigation of the electrocatalytic properties of the fabricated copper micropatterns

Since in recent years there has been active research towards developing non-enzymatic sensors for the detection of different analytes [51-53] held in the human body, the possibility of applying copper micropatterns, as working electrodes for electrochemical sensing of glucose [54-56] has been demonstrated in this work. A study of the electrochemical properties of the fabricated copper micropatterns toward biologically important analytes (e.g. D-glucose) was carried out using cyclic voltammetry and amperometry methods. The deposited copper structures were used as working electrodes for enzyme-free detection of hydrogen peroxide (Fig. 4 a-d) and D-glucose (Fig. 4 e-h).

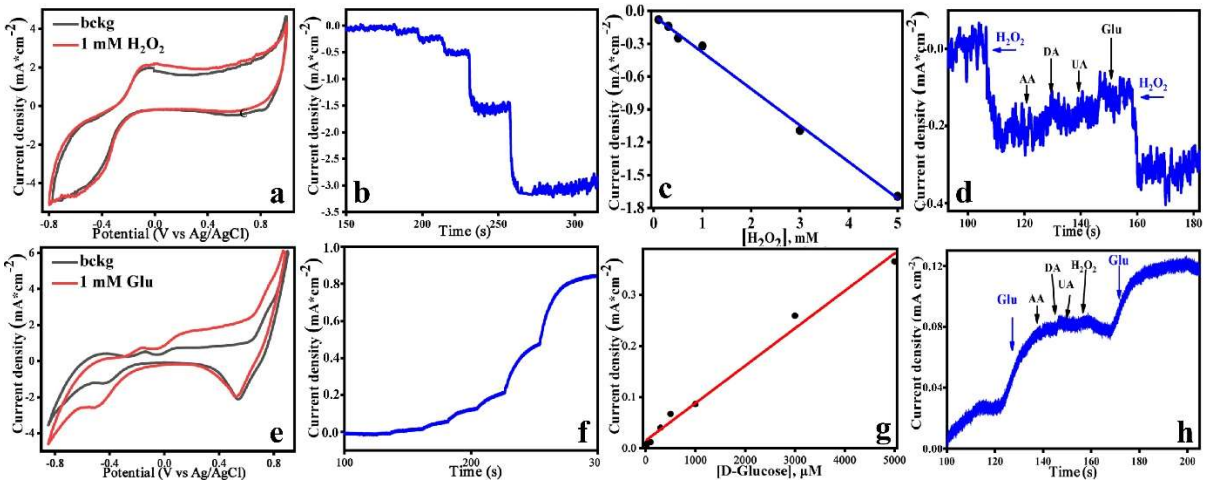

Fig. 4. Cyclic voltammograms of copper electrode recorded in solutions containing hydrogen peroxide (a); Amperogram of copper electrode recorded in solutions containing hydrogen peroxide (b); Linear dependence of the concentration of hydrogen peroxide on the Faraday current (c); Selectivity of the synthesized copper electrode with respect to different interfering agents (d). Cyclic voltammograms of copper electrode recorded in solutions containing D-glucose (e); Amperogram of copper electrode recorded in solutions containing D-glucose (f); Linear dependence of the concentration of D-glucose on the Faraday current (g); Selectivity of the synthesized copper electrode with respect to different interfering agents (h).

In addition, the interfering effect of such interfering substances as urea (UA), paracetamol (AP) and ascorbic acid (AA) was studied (Fig. 4 d, h). Based on amperometric data, the calibration curves for the fabricated copper electrodes were plotted representing the dependences of the Faraday current density on the concentration of the analyte. As a result, such basic sensor characteristics as sensitivity, limit of detection (LOD) and the analyte concentration range corresponding to a linear change of the signal were determined (Table S1 in the supplement).

4. Conclusions

In the current work, we performed rapid laser-induced deposition of copper micropatterns from DES on the surface of oxide glass. It was shown that the use of DES with a copper acetate content of at least 1:0.5 mol/mol (relative to choline chloride) at a laser radiation power in the range of 0,5 -1 W allows the synthesis of copper structures at a scanning speed of up to 2.5 mm s^{-1}. As a result, we demonstrated the possibility of high-rate deposition copper micropatterns on three-dimensional surfaces with good adhesion. This relatively large range of the laser processing parameters can be attributed to the high reflectivity of metallic copper, which stops further temperature increase after the metallic structure appears in the DES.

To determine the optimal chemical composition, calculations were performed to confirm that using citric and tartaric acids and copper acetate would be more advantageous for producing uniform copper-enriched structures under laser radiation. Additionally, assumptions were made about the effect of laser radiation on the process in terms of achieved temperatures.

The fabricated copper material revealed good electrocatalytic activity toward non-enzymatic detection of D-glucose and hydrogen peroxide. Thus, the proposed technology can be successfully used for design and development of new microelectronic devices as well as flexible sensor platforms for electrochemical analysis.

Declarations

Ethical Approval
Not applicable.

Competing interests
The authors declare no conflict of interest.

Author contributions
Conceptualization, I.I.T., E.M.K. and A.Yu.S.; methodology, E.G., E.M.K., E.G. and A.Yu.S.; formal analysis, A.S.L., E.M.K. and V.M.; investigation, D.I.G., E.M.K., L.S.L. and A.K.; data curation, E.M.K., I.Ch. and M.S.P; writing—original draft preparation, E.G., A.Yu.S., E.M.K. and I.I.T.; writing—review and editing, E.G., I.I.T., E.M.K., A.Yu.S., and M.S.P.; visualization, V.B.S., A.K. and A.S.L.; supervision, I.I.T. and E.M.K; project administration, I.I.T. and A.Yu.S.; funding acquisition, I.I.T.
All authors have read and agreed to the published version of the manuscript.

Data and code availability
Not applicable.

Supplementary information
Below is the link to the electronic supplementary material.

Acknowledgments
I.I.T., E.M.K., A.S.L. and M.S.P. acknowledge Russian Science Foundation (grant 20-79-10075). The authors would like to thank the SPbSU Nanotechnology Interdisciplinary Centre, Centre for Physical Methods of Surface Investigation, Centre for Optical and Laser Materials Research and Centre for X-ray Diffraction Studies.

[1] S. Khan, L. Lorenzelli, and R. S. Dahiya, “Technologies for printing sensors and electronics over large flexible substrates: A review,” *IEEE Sens. J.*, vol. 15, no. 6, 2015, doi: 10.1109/JSEN.2014.2375203.
[2] J. Zhang *et al.*, “Laser-Induced Selective Metallization on Polymer Substrates Using Organocopper for Portable Electronics,” *ACS Appl. Mater. Interfaces*, vol. 11, no. 14, 2019, doi: 10.1021/acsami.9b01856.
[3] S. Bai *et al.*, “Laser-assisted reduction of highly conductive circuits based on copper nitrate for flexible printed sensors,” *Nano-Micro Lett.*, vol. 9, no. 4, 2017, doi: 10.1007/s40820-017-0139-3.
[4] V. Binh Nam, T. Thi Giang, and D. Lee, “Laser digital patterning of finely-structured flexible copper electrodes using copper oxide nanoparticle ink produced by a scalable synthesis method,” *Appl. Surf. Sci.*, vol. 570, 2021, doi: 10.1016/j.apsusc.2021.151179.
[5] K. Ratautas, M. Andrulevičius, A. Jagminienė, I. Stankevičienė, E. Norkus, and G. Račiukaitis, “Laser-assisted selective copper deposition on commercial PA6 by catalytic electroless plating – Process and activation mechanism,” *Appl. Surf. Sci.*, vol. 470, 2019, doi: 10.1016/j.apsusc.2018.11.091.
[6] E. M. Khairullina, M. S. Panov, V. S. Andriianov, K. Ratautas, I. I. Tumkin, and G. Račiukaitis, “High rate fabrication of copper and copper-gold electrodes by laser-induced selective electroless plating for enzyme-free glucose sensing,” *RSC Adv.*, vol. 11, no. 32, 2021, doi: 10.1039/d1ra01565f.
[7] K. Ratautas *et al.*, “Laser-induced selective metallization of polypropylene doped with multiwall carbon nanotubes,” *Appl. Surf. Sci.*, vol. 412, 2017, doi: 10.1016/j.apsusc.2017.03.238.
[8] P. Rytlewski *et al.*, “Laser-induced surface activation and electroless metallization of

polyurethane coating containing copper(II) L-tyrosine," *Appl. Surf. Sci.*, vol. 505, 2020, doi: 10.1016/j.apsusc.2019.144429.
[9] P. Rytlewski *et al.*, "Laser activated and electroless metalized polyurethane coatings containing copper(Ii) l-tyrosine and glass microspheres," *Molecules*, vol. 26, no. 18, 2021, doi: 10.3390/molecules26185571.
[10] Y. Huang, X. Xie, M. Li, M. Xu, and J. Long, "Copper circuits fabricated on flexible polymer substrates by a high repetition rate femtosecond laser-induced selective local reduction of copper oxide nanoparticles," *Opt. Express*, vol. 29, no. 3, 2021, doi: 10.1364/oe.416772.
[11] M. Mizoshiri, S. Arakane, J. Sakurai, and S. Hata, "Direct writing of Cu-based micro-temperature detectors using femtosecond laser reduction of CuO nanoparticles," *Appl. Phys. Express*, vol. 9, no. 3, 2016, doi: 10.7567/APEX.9.036701.
[12] L. S. Logunov *et al.*, "Influence of the ligand nature on the in situ laser-induced synthesis of the electrocatalytically active copper microstructures," *Arab. J. Chem.*, vol. 11, no. 5, 2018, doi: 10.1016/j.arabjc.2017.11.003.
[13] D. I. Gordeychuk *et al.*, "Copper-based nanocatalysts produced via laser-induced ex situ generation for homo- and cross-coupling reactions," *Chem. Eng. Sci.*, vol. 227, 2020, doi: 10.1016/j.ces.2020.115940.
[14] M. S. Panov, I. I. Tumkin, A. V. Smikhovskaia, E. M. Khairullina, D. I. Gordeychuk, and V. A. Kochemirovsky, "High rate in situ laser-induced synthesis of copper nanostructures performed from solutions containing potassium bromate and ethanol," *Microelectron. Eng.*, vol. 157, 2016, doi: 10.1016/j.mee.2016.02.014.
[15] I. I. Tumkin *et al.*, "Laser-induced deposition of nanostructured copper microwires on surfaces of composite materials," *Surf. Coatings Technol.*, vol. 264, 2015, doi: 10.1016/j.surfcoat.2014.09.030.
[16] M. S. Panov *et al.*, "Non-enzymatic sensors based on in situ laser-induced synthesis of copper-gold and gold nano-sized microstructures," *Talanta*, vol. 167, 2017, doi: 10.1016/j.talanta.2017.01.089.
[17] V. A. Kochemirovsky, S. V. Safonov, I. I. Tumkin, Y. S. Tver'Yanovich, I. A. Balova, and L. G. Menchikov, "Optimization of the solution composition for laser-induced chemical liquid phase deposition of copper," *Russ. Chem. Bull.*, vol. 60, no. 8, 2011, doi: 10.1007/s11172-011-0232-6.
[18] Y. Y. Cao, N. Takeyasu, T. Tanaka, X. M. Duan, and S. Kawata, "3D metallic nanostructure fabrication by surfactant-assisted multiphoton-induced reduction," *Small*, vol. 5, no. 10, 2009, doi: 10.1002/smll.200801179.
[19] D. V. Mamonova *et al.*, "Laser-induced deposition of plasmonic Ag and Pt nanoparticles, and periodic arrays," *Materials (Basel).*, vol. 14, no. 1, 2021, doi: 10.3390/ma14010010.
[20] P. Barton, S. Mukherjee, J. Prabha, B. W. Boudouris, L. Pan, and X. Xu, "Fabrication of silver nanostructures using femtosecond laser-induced photoreduction," *Nanotechnology*, vol. 28, no. 50, 2017, doi: 10.1088/1361-6528/aa977b.
[21] S. Winter, M. Zenou, and Z. Kotler, "Conductivity of laser printed copper structures limited by nano-crystal grain size and amorphous metal droplet shell," *J. Phys. D. Appl. Phys.*, vol. 49, no. 16, 2016, doi: 10.1088/0022-3727/49/16/165310.
[22] N. Gorodesky *et al.*, "Improving compactness of 3d metallic microstructures printed by laser-induced forward transfer," *Crystals*, vol. 11, no. 3, 2021, doi: 10.3390/cryst11030291.
[23] Z. Ur Rehman, F. Yang, M. Wang, and T. Zhu, "Fundamentals and Advances in Laser-Induced Transfer," *Optics and Laser Technology*, vol. 160. 2023, doi: 10.1016/j.optlastec.2022.109065.
[24] I. I. Tumkin, E. M. Khairullina, M. S. Panov, K. Yoshidomi, and M. Mizoshiri, "Copper and nickel microsensors produced by selective laser reductive sintering for non-enzymatic glucose detection," *Materials (Basel).*, vol. 14, no. 10, 2021, doi: 10.3390/ma14102493.
[25] M. Mizoshiri, K. Nishitani, and S. Hata, "Effect of heat accumulation on femtosecond laser reductive sintering of mixed CuO/NiO nanoparticles," *Micromachines*, vol. 9, no. 6, 2018,

doi: 10.3390/mi9060264.
[26] I. Theodorakos, F. Zacharatos, R. Geremia, D. Karnakis, and I. Zergioti, “Selective laser sintering of Ag nanoparticles ink for applications in flexible electronics,” in *Applied Surface Science*, 2015, vol. 336, doi: 10.1016/j.apsusc.2014.10.120.
[27] K. Ratautas, V. Vosylius, A. Jagminienė, I. Stankevičienė, E. Norkus, and G. Račiukaitis, “Laser-induced selective electroless plating on pc/abs polymer: Minimisation of thermal effects for supreme processing speed,” *Polymers (Basel).*, vol. 12, no. 10, 2020, doi: 10.3390/polym12102427.
[28] K. Ratautas, A. Jagminienė, I. Stankevičienė, M. Sadauskas, E. Norkus, and G. Račiukaitis, “Evaluation and optimisation of the SSAIL method for laser-assisted selective electroless copper deposition on dielectrics,” *Results Phys.*, vol. 16, 2020, doi: 10.1016/j.rinp.2020.102943.
[29] M. S. Panov, E. M. Khairullina, F. S. Vshivtcev, M. N. Ryazantsev, and I. I. Tumkin, “Laser-induced synthesis of composite materials based on iridium, gold and platinum for non-enzymatic glucose sensing,” *Materials (Basel).*, vol. 13, no. 15, 2020, doi: 10.3390/ma13153359.
[30] A. V. Smikhovskaia *et al.*, “In situ laser-induced synthesis of copper-silver microcomposite for enzyme-free D-glucose and L-alanine sensing,” *Appl. Surf. Sci.*, vol. 488, 2019, doi: 10.1016/j.apsusc.2019.05.061.
[31] A. V. Smikhovskaia *et al.*, “In situ laser-induced codeposition of copper and different metals for fabrication of microcomposite sensor-active materials,” *Anal. Chim. Acta*, vol. 1044, 2018, doi: 10.1016/j.aca.2018.07.042.
[32] A. S. Levshakova *et al.*, “Modification of nickel micropatterns for sensor-active applications from deep eutectic solvents,” *Opt. Quantum Electron.*, vol. 55, no. 3, 2023, doi: 10.1007/s11082-022-04403-2.
[33] A. Shishov *et al.*, “Laser-induced deposition of copper from deep eutectic solvents: Optimization of chemical and physical parameters,” *New J. Chem.*, vol. 45, no. 46, 2021, doi: 10.1039/d1nj04158d.
[34] A. S. Levshakova *et al.*, “Highly rapid direct laser fabrication of Ni micropatterns for enzyme-free sensing applications using deep eutectic solvent,” *Mater. Lett.*, vol. 308, 2022, doi: 10.1016/j.matlet.2021.131085.
[35] E. L. Smith, A. P. Abbott, and K. S. Ryder, “Deep Eutectic Solvents (DESs) and Their Applications,” *Chemical Reviews*, vol. 114, no. 21. 2014, doi: 10.1021/cr300162p.
[36] B. B. Hansen *et al.*, “Deep Eutectic Solvents: A Review of Fundamentals and Applications,” *Chemical Reviews*, vol. 121, no. 3. 2021, doi: 10.1021/acs.chemrev.0c00385.
[37] L. I. N. Tomé, V. Baião, W. da Silva, and C. M. A. Brett, “Deep eutectic solvents for the production and application of new materials,” *Applied Materials Today*, vol. 10. 2018, doi: 10.1016/j.apmt.2017.11.005.
[38] A. Shishov, D. Gordeychuk, L. Logunov, and I. Tumkin, “High rate laser deposition of conductive copper microstructures from deep eutectic solvents,” *Chem. Commun.*, vol. 55, no. 65, 2019, doi: 10.1039/c9cc05184h.
[39] F. Neese, F. Wennmohs, U. Becker, and C. Riplinger, “The ORCA quantum chemistry program package,” *J. Chem. Phys.*, vol. 152, no. 22, 2020, doi: 10.1063/5.0004608.
[40] W. R. Fawcett, “The ionic work function and its role in estimating absolute electrode potentials,” *Langmuir*, vol. 24, no. 17, 2008, doi: 10.1021/la7038976.
[41] C. L. Altan, B. Gurten, N. A. J. M. Sommerdijk, and S. Bucak, “Deterioration in effective thermal conductivity of aqueous magnetic nanofluids,” *J. Appl. Phys.*, vol. 116, no. 22, 2014, doi: 10.1063/1.4902441.
[42] N. Albayati, M. Kadhom, G. Abdullah, and S. Salih, “Thermal Conductivity of Room Temperature Deep Eutectic Solvents,” *J. Therm. Sci.*, vol. 30, no. 6, 2021, doi: 10.1007/s11630-021-1428-1.
[43] H. Landaluce, L. Arjona, A. Perallos, F. Falcone, I. Angulo, and F. Muralter, “A review of iot sensing applications and challenges using RFID and wireless sensor networks,” *Sensors*

(Switzerland), vol. 20, no. 9. 2020, doi: 10.3390/s20092495.
[44] T. Someya and M. Amagai, "Toward a new generation of smart skins," *Nat. Biotechnol.*, vol. 37, no. 4, 2019, doi: 10.1038/s41587-019-0079-1.
[45] B. Le Borgne, O. De Sagazan, S. Crand, E. Jacques, and M. Harnois, "Conformal Electronics Wrapped Around Daily Life Objects Using an Original Method: Water Transfer Printing," *ACS Appl. Mater. Interfaces*, vol. 9, no. 35, 2017, doi: 10.1021/acsami.7b07327.
[46] H. Tao *et al.*, "Silk-based conformal, adhesive, edible food sensors," *Adv. Mater.*, vol. 24, no. 8, p. Tao, H., Brenckle, M. A., Yang, M., Zhang, J., Liu, 2012, doi: 10.1002/adma.201103814.
[47] S. Hou, J. Liu, F. Shi, G. X. Zhao, J. W. Tan, and G. Wang, "Recent Advances in Silver Nanowires Electrodes for Flexible Organic/Perovskite Light-Emitting Diodes," *Frontiers in Chemistry*, vol. 10. 2022, doi: 10.3389/fchem.2022.864186.
[48] Y. T. Li *et al.*, "Review on Organic-Inorganic Two-Dimensional Perovskite-Based Optoelectronic Devices," *ACS Applied Electronic Materials*, vol. 4, no. 2. 2022, doi: 10.1021/acsaelm.1c00781.
[49] D. Lloyd, T. Vainikka, L. Murtomäki, K. Kontturi, and E. Ahlberg, "The kinetics of the Cu2+/Cu+ redox couple in deep eutectic solvents," *Electrochim. Acta*, vol. 56, no. 14, 2011, doi: 10.1016/j.electacta.2011.03.133.
[50] P. De Vreese *et al.*, "Speciation of copper(II) complexes in an ionic liquid based on choline chloride and in choline chloride/water mixtures," *Inorg. Chem.*, vol. 51, no. 9, 2012, doi: 10.1021/ic202341m.
[51] T. Lin, Y. Xu, A. Zhao, W. He, and F. Xiao, "Flexible electrochemical sensors integrated with nanomaterials for in situ determination of small molecules in biological samples: A review," *Analytica Chimica Acta*, vol. 1207. 2022, doi: 10.1016/j.aca.2022.339461.
[52] F. Yuan, Y. Xia, Q. Lu, Q. Xu, Y. Shu, and X. Hu, "Recent advances in inorganic functional nanomaterials based flexible electrochemical sensors," *Talanta*, vol. 244. 2022, doi: 10.1016/j.talanta.2022.123419.
[53] Y. Luo, C. Fan, Y. Song, T. Xu, and X. Zhang, "Ultra-trace enriching biosensing in nanoliter sample," *Biosens. Bioelectron.*, vol. 210, 2022, doi: 10.1016/j.bios.2022.114297.
[54] D. Bruen, C. Delaney, L. Florea, and D. Diamond, "Glucose sensing for diabetes monitoring: Recent developments," *Sensors (Switzerland)*, vol. 17, no. 8. 2017, doi: 10.3390/s17081866.
[55] H. Lee *et al.*, "Wearable/disposable sweat-based glucose monitoring device with multistage transdermal drug delivery module," *Sci. Adv.*, vol. 3, no. 3, 2017, doi: 10.1126/sciadv.1601314.
[56] T. Lin, "Non-Invasive Glucose Monitoring: A Review of Challenges and Recent Advances," *Curr. Trends Biomed. Eng. Biosci.*, vol. 6, no. 5, 2017, doi: 10.19080/ctbeb.2017.06.555696.